

Stress-Based Finite Element Methods for Dynamics Analysis of Euler-Bernoulli Beams with Various Boundary Conditions

Abstract

In this research, two stress-based finite element methods including the curvature-based finite element method (CFE) and the curvature-derivative-based finite element method (CDFE) are developed for dynamics analysis of Euler-Bernoulli beams with different boundary conditions. In CFE, the curvature distribution of the Euler-Bernoulli beams is approximated by its nodal curvatures then the displacement distribution is obtained by its integration. In CDFE, the displacement distribution is approximated in terms of nodal curvature derivatives by integration of the curvature derivative distribution. In the introduced methods, compared with displacement-based finite element method (DFE), not only the required number of degrees of freedom is reduced, but also the continuity of stress at nodal points is satisfied. In this paper, the natural frequencies of beams with different type of boundary conditions are obtained using both CFE and CDFE methods. Furthermore, some numerical examples for the static and dynamic response of some beams are solved and compared with those obtained by DFE method.

Keywords

Euler-Bernoulli beams, Stress-based finite element, Natural frequency, Dynamic analysis.

Majid Gholampour ^a

Bahman Nouri Rahmat Abadi ^{a,*}

Mehrdad Farid ^a

William L. Cleghorn ^b

^a School of Mechanical Engineering, Shiraz University, Shiraz, Iran.

^b Department of mechanical and industrial Engineering, University of Toronto, Toronto, Ontario, Canada.

*Corresponding author: E-mail: bahmannouri@shirazu.ac.ir

<http://dx.doi.org/10.1590/1679-78253927>

Received 12.04.2017

Accepted 16.06.2017

Available online 17.06.2017

1 INTRODUCTION

Displacement-based finite element (DFE) method has extensively been used in computational solid mechanics. In this method, the displacement and slope are used as the nodal values in the modelling of beams. The main disadvantage of DFE is the discontinuity in the stress distribution. Furthermore, stress boundary conditions are not exactly satisfied which causes the inaccuracy of the approximated solution. To eliminate the mentioned problem, stress-based finite element (SFE) has been introduced (De Veubeke, 1965; De Veubeke, 1967). In this method, stress distribution is approximated by assumed stress function and the transverse deflections and slopes are obtained by

integration. Consequently, the considered method provides the continuities of not only transverse deflection but also stress at nodes. This technique was used for analyzing different problems, such as Kirchhoff plates (Morley, 1968; Punch and Atluri, 1986), plane elastic problems (Watwood and Hartz, 1968; Wieckowski et al., 1999) and elasto-plastic analysis (Wieckowski, 1995; Kuo et al., 2006).

Kuo et al. (2006) introduced CFE method for Euler- Bernoulli beam. In their work (Kuo et al., 2006), a cantilever beam and a slewing beam were studied. After that, they used CFE (Kuo and Cleghorn, 2011) and SFE method (Kuo and Cleghorn, 2007) to study a four-bar mechanism and a flexible slider crank mechanism with small strain but large rigid body motion, respectively.

Later, Farid and Cleghorn (2012) utilized CFE method for the first time to model the dynamics of a single-flexible-link spatial manipulator. They also obtained the dynamic equations of planar multi flexible-link manipulators and verified the results with the displacement finite element method (Farid and Cleghorn, 2014). Furthermore, an improved curvature-based finite element method was developed in (Chen et al., 2015) for the dynamic modelling of a high-speed planar parallel manipulator with flexible links. Also, the method was used for solving a sliding beam problem (Kuo, 2015). The varying-length beam element was established for solving the considered problem.

To the best of our knowledge, the CFE method has been used for the analysis of the problems in which the beams are considered to be clamped-free. The main scope of the present research is to extend the CFE and to introduce CDFE method for vibration analysis of Euler-Bernoulli beams with different boundary conditions.

The paper is organized as follows: Section 2 introduces both stress-based finite element methods. In section 3, the shape functions of both CFE and CDFE methods are obtained for different boundary conditions in order to approximate the deflection in each element. In section 4, using Lagrange's equation, equations of motion are obtained and the natural frequencies of beams are obtained. Finally, in section 5, numerical examples related to the static and dynamic responses of some beams are investigated.

2 STRESS-BASED FINITE ELEMENT METHODS

In Figure 1, the Euler-Bernoulli beam divided into N element is depicted. The transverse deflection, slope and the nodal variable at the left end of the e th element are designated with w_1^e, ψ_1^e and v_1^e , while those at the right end are shown with, w_2^e, ψ_2^e and v_{e+1}^e , respectively. Also, the i th global nodal variable, v_i in each of CFE and CDFE methods are considered m_i and n_i , respectively.

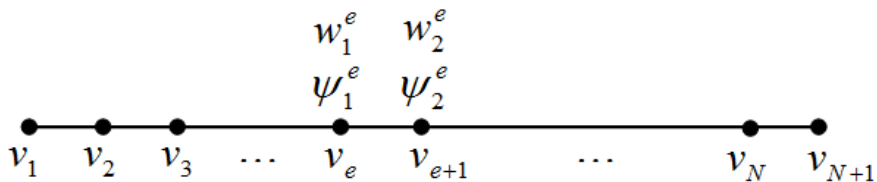


Figure 1: An Euler-Bernoulli beam element.

In sequence, the shape functions in each of the curvature and the curvature derivative-based finite element methods are obtained.

2.1 Curvature-Based Finite Element Method (CFE)

The curvature distribution in the e th element, $m^e(\xi)$, can be linearly approximated as

$$m^e(\xi) = S_1(\xi)m_1^e + S_2(\xi)m_2^e \tag{1}$$

where, $S_1(\xi)$ and $S_2(\xi)$ are considered as

$$S_1(\xi) = 1 - \xi \quad , \quad S_2(\xi) = \xi \tag{2}$$

in which

$$\xi = (x - x_e) / (x_{e+1} - x_e) \tag{3}$$

The slope in the e th element, ψ^e can be obtained by integrating Eq. (1).

$$\psi^e(\xi) = h_e \left[\left(\xi - \frac{\xi^2}{2} \right) m_1^e + \frac{\xi^2}{2} m_2^e + c_1^e \right] \tag{4}$$

where, c_1^e is a constant. Considering the slope of the first node as ψ_0 , the constant can be written as

$$c_1^e = \frac{\psi_0}{h_1} \tag{5}$$

Using the continuity of slope between the first and the second element, the constant, c_1^2 is derived as

$$c_1^2 = \frac{1}{h_2^2} \left[\frac{1}{2} h_1 h_2 m_1 + \frac{1}{2} h_1 h_2 m_2 + h_2 \psi_0 \right] \tag{6}$$

In general, the constant c_1^e for the e th element can be obtained in a similar way as

$$c_1^e = \frac{1}{h_e^2} \left[\frac{1}{2} h_1 h_e m_1 + \left(\frac{1}{2} h_1 h_e + \frac{1}{2} h_2 h_e \right) m_2 + \left(\frac{1}{2} h_2 h_e + \frac{1}{2} h_3 h_e \right) m_3 + \dots + \left(\frac{1}{2} h_{e-2} h_e + \frac{1}{2} h_{e-1} h_e \right) m_{e-1} + \frac{1}{2} h_{e-1} h_e m_e + h_2 \psi_0 \right] \tag{7}$$

Integrating Eq. (4), the transverse deflection in the e th element can be obtained by the following equation.

$$w^e(\xi) = h_e^2 \left[\left(\frac{\xi^2}{2} - \frac{\xi^3}{6} \right) m_1^e + \frac{\xi^3}{6} m_2^e + c_1^e \xi + c_2^e \right] \tag{8}$$

In Eq. (8), c_2^e is a constant parameter determined by boundary conditions. Considering the continuity of deflection at the internal nodes, the constant is obtained as

$$c_2^e = \frac{1}{h_e^2} \left[\frac{1}{2} h_1^2 m_1 + \left(\frac{1}{6} h_1^2 + \frac{1}{3} h_2^2 \right) m_2 + \left(\frac{1}{6} h_2^2 + \frac{1}{3} h_3^2 \right) m_3 + \dots + \left(\frac{1}{6} h_{e-2}^2 + \frac{1}{3} h_{e-1}^2 \right) m_{e-1} + \frac{1}{6} h_{e-1}^2 m_e + h_1^2 c_1^1 + h_2^2 c_1^2 + \dots + h_{e-1}^2 c_1^{e-1} + c_2^1 \right] \tag{9}$$

Using Eqs. (7-9), the deflection of the e th element is approximated as

$$w^e(\xi) = \sum_{i=1}^{N+1} H_i^e(\xi) m_i + N_1^e \psi_0 + N_2^e w_0 \tag{10}$$

In the above relation, $H_i^e(\xi)$, N_1^e and N_2^e are the shape functions of the e th element obtained as

For $e = 1$

$$H_1^1 = h_1^2 \left(\frac{\xi^2}{2} - \frac{\xi^3}{6} \right) \tag{11-a}$$

For $e = 3, 4, \dots, N$

$$H_1^e = \frac{h_1^2}{3} + \frac{h_1}{2} \sum_{k=2}^{e-1} h_k + \frac{h_1 h_e}{2} \xi \tag{11-b}$$

For $e = 1, 2, \dots, N$

$$H_{e+1}^e = \frac{h_e^2}{6} \xi \tag{11-c}$$

For $e = 2, 3, \dots, N$

$$H_e^e = \frac{h_{e-1}^2}{6} + \frac{h_{e-1} h_e}{2} \xi + h_e^2 \left(\frac{\xi^2}{2} - \frac{\xi^3}{6} \right) \tag{11-d}$$

For $e = 3, 4, \dots, N$

$$H_{e-1}^e = \frac{h_{e-2}^2}{6} + \frac{h_{e-2} h_{e-1}}{2} + \frac{h_{e-1}^2}{2} + h_e \left(\frac{h_{e-2} + h_{e-1}}{2} \right) \xi \tag{11-e}$$

For $e = 4, 5, \dots, N$

$$H_{e-2}^e = \frac{h_{e-3}^2}{6} + \frac{h_{e-3} h_{e-2}}{2} + \frac{h_{e-2}^2}{3} + h_{e-1} \left(\frac{h_{e-3} + h_{e-2}}{2} \right) + h_e \left(\frac{h_{e-3} + h_{e-2}}{2} \right) \xi \tag{11-f}$$

For $i = e + 2, \dots, N + 1$

$$H_i^e = 0 \tag{11-g}$$

where, N is the total number of elements. Also, N_1^e and N_2^e are derived as

$$N_1^e = h_e \xi + (h_1 + h_2 + \dots + h_{e-1}) \tag{12-a}$$

$$N_2^e = 1 \tag{12-b}$$

2.2 Curvature Derivative-Based Finite Element Method (CDFE)

The curvature derivative distribution in the e th element, $n^e(\xi)$, can be linearly approximated as

$$v^e(\xi) = S_1(\xi)n_1^e + S_2(\xi)n_2^e \tag{13}$$

where, $S_1(\xi)$ and $S_2(\xi)$ are defined in Eq. (2). The curvature distribution in the beam can be obtained by integrating Eq. (13).

$$m^c(\xi) = h_e \left[\left(\xi - \frac{\xi^2}{2} \right) n_1^c + \frac{\xi^2}{2} n_2^c + c_1^c \right] \tag{14}$$

The slope and transverse deflection of the e th element can be obtained by integrating Eq. (14) as

$$\psi^e(\xi) = h_e^2 \left[\left(\frac{\xi^2}{2} - \frac{\xi^3}{6} \right) n_1^c + \frac{\xi^3}{6} n_2^c + c_1^e \xi + c_2^e \right] \tag{15}$$

$$w^e(\xi) = h_e^3 \left[\left(\frac{\xi^3}{6} - \frac{\xi^4}{24} \right) n_1^c + \frac{\xi^4}{24} n_2^c + c_1^e \frac{\xi^2}{2} + c_2^e \xi + c_3^e \right] \tag{16}$$

in which, c_1^e , c_2^e and c_3^e are the constant parameters obtained by the continuity of curvature, slope and deflection between elements. The constants c_1^e and c_2^e are similar to the CFE method and the constant c_3^e is derived given as

$$\begin{aligned} c_3^e = & \frac{1}{h_e^3} \left[\left(\frac{h_1^2}{3} + \frac{h_1}{4} + \frac{h_1}{2} \sum_{k=1}^{e-1} h_k \right) n_1 + \left(\frac{1}{6} h_1^2 + \frac{1}{3} h_2^2 + \left[\frac{1}{6} + \frac{3}{4}(e-4) \right] + \sum_{k=5}^{e-1} \left[\left(\frac{1}{2} + (e-k) \frac{1}{2} \right) h_{k-2} \right] \right) [h_1 + h_2] n_2 \right. \\ & + \left(\frac{1}{6} h_1^2 + \frac{1}{3} h_2^2 + \left[\frac{1}{6} + \frac{3}{4}(e-4) \right] + \sum_{k=6}^{e-1} \left[\left(\frac{1}{2} + (e-k) \frac{1}{2} \right) h_{k-2} \right] \right) [h_1 + h_2] n_3 + \dots \\ & + \left(\frac{1}{6} h_1^2 + \frac{1}{3} h_2^2 + \left[\frac{1}{6} + \frac{3}{4}(e-4) \right] + \sum_{k=5}^{e-1} \left[\left(\frac{1}{2} + (e-k) \frac{1}{2} \right) h_{k-2} \right] \right) [h_1 + h_2] n_{e-1} \\ & \left. + \left(\frac{h_e^3}{8} + \frac{h_{e-1}^2}{6} + \frac{h_{e-2}}{4} \right) n_e + \frac{h_e^3}{24} n_{e+1} \right] \end{aligned} \tag{17}$$

The deflection of the e th element in the CDFE method can be written as

$$w^e(\xi) = \sum_{i=1}^{N+1} H_i^e(\xi) n_i + N_1^e m_0 + N_2^e \psi_0 + N_3^e w_0 \tag{18}$$

in which, the shape functions $H_i^e(\xi)$ are obtained as

For $e = 1$

$$H_1^1 = h_1^3 \left(\frac{\xi^3}{6} - \frac{\xi^4}{24} \right) \tag{19-a}$$

For $e = 3, 4, \dots, N$

$$H_1^e = \frac{h_1^3}{8} + \frac{h_1^2}{3} \xi + \frac{h_1}{4} \xi^2 + \left(\frac{h_1}{2} \sum_{k=2}^{e-1} h_k \right) \xi + \frac{(e-1)}{4} h_1 \tag{19-b}$$

For $e = 1, 2, \dots, N$

$$H_{e+1}^e = \frac{h_e^3}{24} \xi^4 \tag{19-c}$$

For $e = 2, 3, \dots, N$

$$H_e^e = \frac{h_{e-1}^3}{24} + \frac{h_{e-1}^2}{6} \xi + \frac{h_{e-1}}{4} \xi^2 + h_e^3 \left(\frac{\xi^3}{6} - \frac{\xi^4}{24} \right) \tag{19-d}$$

For $e = 3, 4, \dots, N$

$$H_{e-1}^e = \frac{h_{e-2}^3}{24} + \frac{h_{e-1}^3}{8} + \frac{h_{e-2}^2}{6} + \frac{h_{e-1}}{4} + \frac{h_{e-2}^2}{6} \xi + \frac{h_{e-1}^2}{3} \xi + \frac{h_{e-2} h_{e-1}}{6} \xi + \frac{h_{e-1}}{4} \xi^2 + \frac{h_{e-2}}{12} \xi^2 \tag{19-e}$$

For $e = 4, 5, \dots, N$

$$H_{e-2}^e = \frac{h_{e-3}^3}{24} + \frac{h_{e-2}^3}{8} + \frac{h_{e-3}^2}{3} + \frac{h_{e-3} h_{e-2}}{6} + \frac{h_{e-3}}{3} + \frac{h_{e-1}}{4} + \frac{h_{e-3}^2}{6} \xi + \frac{h_{e-2}^2}{3} \xi + \frac{h_{e-2} h_{e-3}}{2} \xi + h_e \left(\frac{h_{e-3} + h_{e-2}}{2} \right) \xi + \left(\frac{h_{e-3} + h_{e-2}}{4} \right) \xi^2 \tag{19-f}$$

For $i = e + 2, \dots, N + 1$

$$H_i^e = 0 \tag{19-g}$$

Furthermore, N_1^e , N_2^e and N_3^e are derived as

$$N_1^e = \frac{1}{2} h_e \xi^2 + (h_1 + h_2 + \dots + h_{e-1}) \xi + \frac{(e-1)^2}{2} \tag{20-a}$$

$$N_2^e = h_e \xi + (h_1 + h_2 + \dots + h_{e-1}) \tag{20-b}$$

$$N_3^e = 1 \tag{20-c}$$

In the appendix, the first five shape functions in the CFE and CDFE methods are given.

3 BEAMS WITH DIFFERENT BOUNDARY CONDITIONS

In this section, the unknown constants in Eqs, (10) and (18) are obtained by considering the boundary conditions. In CFE method, two of the boundary conditions are used to determine the constants ψ_0 and w_0 , the other boundary conditions are incorporated as constraints. In CDFE method, the constant m_0 , ψ_0 and w_0 are obtained by using three boundary conditions and the other one is imposed as constraint.

Therefore, the deflection of the elements in the CFE and CDFE methods can be written in terms of nodal variables as

$$w^e(\xi) = \sum_{i=1}^{N+1} \bar{H}_i^e(\xi) v_i \tag{21}$$

In what follows, the shape functions, $\bar{H}_i^e(\xi)$ in the CFE and CDFE methods are obtained for different boundary conditions such as clamped-free, pinned-pinned, pinned-guided, clamped-pinned, clamped-guided and clamped-clamped.

3.1 Clamped Free (CFE)

For the clamped free beam, the deflection and slope of the first node are zero and the boundary conditions are written as

$$w^1(\xi = 0) = \psi^1(\xi = 0) = 0 \tag{22}$$

Thus, ψ_0 and w_0 are zero and the shape function \bar{H}_i^e are obtained the same as H_i^e .

3.2 Clamped Free (CDFE)

For the clamped free beam, the constants w_0 , ψ_0 and m_0 in Eq. (18), are obtained using the following conditions

$$w^1(\xi = 0) = \psi^1(\xi = 0) = m^N(\xi = 1) = 0 \tag{23}$$

Constants ψ_0 and w_0 are zero and the following relation for m_0 is derived

$$m_0 = -\frac{1}{N_1^{nN}(\xi = 1)} [H_1^{nN}(\xi = 1)n_1 + H_2^{nN}(\xi = 1)n_2 + \dots + H_{N+1}^{nN}(\xi = 1)n_{N+1}] \tag{24}$$

Therefore, the shape functions can be presented in the form of Eq. (21), where \bar{H}_i^e is obtained as

$$\bar{H}_i^e = H_i^e - \frac{1}{N_1^{nN}(\xi = 1)} N_1^e H_i^{ne}(\xi = 1) \quad i = 1, 2, \dots, N + 1 \tag{25}$$

3.3 Pinned-Pinned (CFE)

In this case, the boundary conditions are given as

$$w^l(\xi=0) = w^N(\xi=1) = 0 \quad (26)$$

Considering the first boundary condition, constant w_0 is zero. Incorporating, the second boundary condition, constant ψ_0 is obtained as

$$\psi_0 = -\frac{1}{N_1^e(\xi=1)} [H_1^e(\xi=1)m_1 + H_2^e(\xi=1)m_2 + \dots + H_{N+1}^e(\xi=1)m_{N+1}] \quad (27)$$

By substituting Eq. (27), to Eq. (10), the deflection of the nodes is obtained in which the shape function, \bar{H}_i^e is obtained as

$$\bar{H}_i^e = H_i^e - \frac{1}{N_1^e(\xi=1)} N_1^N H_i^N(\xi=1) \quad i = 1, 2, \dots, N+1 \quad (28)$$

3.4 Pinned-Pinned (CDFE)

Since the deflection and the curvature at the left side of the beam are zero, constants w_0 and m_0 are zero. Constant ψ_0 can be obtained by considering zero deflection at the left side of the beam as

$$\psi_0 = -\frac{1}{N_1^N(\xi=1)} [H_1^N(\xi=1)n_1 + H_2^N(\xi=1)n_2 + \dots + H_{N+1}^N(\xi=1)n_{N+1}] \quad (29)$$

In this case, the deflection of the beam can be written in the form of Eq. (21), where \bar{H}_i^e is obtained similar to the pinned-pinned beam in CFE method given in Eq. (28).

3.5 Pinned-Guided (CFE)

For the pinned-guided case, the boundary condition are written as

$$w^l(\xi=0) = w'^N(\xi=1) = 0 \quad (30)$$

Considering the boundary conditions, the unknown parameter, w_0 is zero and the parameter ψ_0 is derived as

$$\psi_0 = -\frac{1}{N_1'^e(\xi=1)} [H_1'^e(\xi=1)m_1 + H_2'^e(\xi=1)m_2 + \dots + H_{N+1}'^e(\xi=1)m_{N+1}] \quad (31)$$

Using Eqs. (31), and (10), the nodes' displacement of the pinned-guided beam is derived where, \bar{H}_i^e is obtained as

$$\bar{H}_i^e = H_i^e - \frac{1}{N_1'^e(\xi=1)} N_1'^N H_i'^N(\xi=1) \quad i = 1, 2, \dots, N+1 \quad (32)$$

3.6 Pinned-Guided (CDFE)

Considering the following conditions

$$w^I(\xi=0) = m^I(\xi=1) = w'^N(\xi=1) = 0 \quad (33)$$

Constants w_0 and ψ_0 are zero and m_0 is derived obtained as

$$m_0 = -\frac{1}{N_1'^N(\xi=1)} \left[H_1'^N(\xi=1)n_1 + H_2'^N(\xi=1)n_2 + \dots + H_{N+1}'^N(\xi=1)n_{N+1} \right] \quad (34)$$

In this case, the shape functions can be derived as given in Eq. (32).

3.7 Clamped-Pinned (CFE)

Considering zero deflection and slope for the first node, the shape functions are obtained similar to the clamped free beam in the CFE method. The zero displacement at the right end is considered as a constraint where can be obtained by multiplying the matrix Γ by the vector of curvature. The matrix Γ is given as

$$\Gamma = \left[\bar{H}_1^N(\xi=1) \quad \dots \quad \bar{H}_{N+1}^N(\xi=1) \right] \quad (35)$$

3.8 Clamped-Pinned (CDFE)

Using the following conditions

$$w^I(\xi=0) = w'^N(\xi=1) = w^N(\xi=1) = 0 \quad (36)$$

Constants w_0 and ψ_0 are zeros and m_0 is found as

$$m_0 = -\frac{1}{N_1^N(\xi=1)} \left[H_1^N(\xi=1)n_1 + H_2^N(\xi=1)n_2 + \dots + H_{N+1}^N(\xi=1)n_{N+1} \right] \quad (37)$$

By substituting Eq. (37), to Eq. (18), the deflection of the nodes is obtained in the form of Eq. (28).

3.9 Clamped-Guided (CFE)

In this case, the shape functions are similar to the clamped-free beam in CFE method. Also, the zeros slope at the right end of the beam is considered as a constraint. In this case, the matrix Γ is defined as

$$\Gamma = \left[\bar{H}_1'^N(\xi=1) \quad \dots \quad \bar{H}_{N+1}'^N(\xi=1) \right] \quad (38)$$

3.10 Clamped-Guided (CDFE)

In this case, the constants w_0 , ψ_0 and m_0 are obtained using the following conditions

$$w^1(\xi=0) = w^1(\xi=1) = w'^N(\xi=1) = 0 \quad (39)$$

Constants w_0 and ψ_0 are zero and m_0 is derived as

$$m_0 = -\frac{1}{N_1'^N(\xi=1)} \left[H_1'^N(\xi=1)n_1 + H_2'^N(\xi=1)n_2 + \dots + H_{N+1}'^N(\xi=1)n_{N+1} \right] \quad (40)$$

The shape functions are similar to Eq. (32).

3.11 Clamped-Clamped (CFE)

For beams with this boundary condition, the shape functions are similar to those of the clamped-free beam in CFE method. Furthermore, the constraints are zero displacement and zero slope at the right end of the beam which can be obtained by multiplication the matrix Γ to the curvature vector. In this case, matrix Γ can be presented as

$$\Gamma = \begin{bmatrix} \bar{H}_1^N(\xi=1) & \bar{H}_2^N(\xi=1) & \dots & \bar{H}_{N+1}^N(\xi=1) \\ \bar{H}_1'^N(\xi=1) & \bar{H}_2'^N(\xi=1) & \dots & \bar{H}_{N+1}'^N(\xi=1) \end{bmatrix} \quad (41)$$

3.12 Clamped-Clamped (CDFE)

In this case, the conditions are

$$w^1(\xi=0) = w^1(\xi=1) = w^N(\xi=0) = w'^N(\xi=1) = 0 \quad (42)$$

Constants w_0 and ψ_0 are zero and m_0 is obtained as

$$m_0 = -\frac{1}{N_1^N(\xi=1)} \left[H_1^N(\xi=1)n_1 + H_2^N(\xi=1)n_2 + \dots + H_{N+1}^N(\xi=1)n_{N+1} \right] \quad (43)$$

The zero slope at the right side of the beam is considered as a constraint which, can be obtained by multiplying matrix Γ by curvature derivative vector

$$\Gamma = \left[\bar{H}_1'^N(\xi=1) \quad \bar{H}_2'^N(\xi=1) \quad \dots \quad \bar{H}_{N+1}'^N(\xi=1) \right] \quad (44)$$

The shape functions can be seen in Eq. (28).

4 FREQUENCY EQUATION

In this section, using Lagrange's equation and the assumed deflection of the eth element in terms of nodal curvatures and curvature derivatives in CFE and CDFE methods, respectively, the mass matrix and stiffness matrix can be obtained.

4.1 Mass Matrix

The kinetic energy of the eth beam element can be written as

$$T^e = \frac{1}{2} \rho A \int_0^1 \left(\frac{\partial w^e}{\partial t} \right)^2 d\xi \tag{45}$$

where, the density and the cross area of the beam are designated with constants ρ and A , respectively. Using Eqs. (21) and (45), the kinetic energy can be rewritten as

$$T^e = \frac{1}{2} \rho A \sum_{i=1}^{N+1} \sum_{j=1}^{N+1} \int_0^1 \bar{H}_i^e \bar{H}_j^e \dot{v}_i \dot{v}_j d\xi \tag{46}$$

Thus, the components of the e th element mass matrix are

$$m_{ij}^e = \rho A \int_0^1 \bar{H}_i^e \bar{H}_j^e d\xi \tag{47}$$

Also, the kinetic energy of a beam carrying a concentrated mass, m_0 attached at the e th global node is given as

$$T = \frac{1}{2} m_0 \sum_{i=1}^{N+1} \sum_{j=1}^{N+1} \bar{H}_i^e(\xi=1) \bar{H}_j^e(\xi=1) \dot{v}_i \dot{v}_j \tag{48}$$

Therefore, the corresponding components of the e th element mass matrix can be obtained as

$$m_{ij}^e = m_0 \bar{H}_i^e(\xi=1) \bar{H}_j^e(\xi=1) \tag{49}$$

4.2 Stiffness Matrix

The potential energy of the e th element of the Euler beam can be written as

$$U^e = \frac{1}{2} \int_0^1 EI^e \left[\frac{\partial^2 w^e}{\partial \xi^2} \right]^2 d\xi \tag{50}$$

in which, EI^e is the flexural stiffness of the e th element. Considering the transverse deflection of the e th element, the component of the e th element stiffness matrix can be obtained as

$$k_{ij}^e = \int_0^1 EI^e \bar{H}_i^{''e} \bar{H}_j^{''e} d\xi \tag{51}$$

where, $\bar{H}_i^{''e}$ is the second derivative of \bar{H}_i^e .

If linear and torsional springs with stiffness k_l and k_t are attached to the e th global node, the corresponding component of the stiffness matrix can be obtained as

$$k_{ij}^e = k_l \bar{H}_i^e(\xi=1) \bar{H}_j^e(\xi=1) + k_t \bar{H}_i^{'e}(\xi=1) \bar{H}_j^{'e}(\xi=1) \tag{52}$$

Remark: The size of the total mass and stiffness matrices of the spring-mass-beam system is $(e+1) \times (e+1)$. The ij mponent of the assembled mass and stiffness matrix is obtained by summation of all the ij component of elemental mass and stiffness matrices.

4.3 Load Vector

The virtual work of a discrete load, F_k acting at the e th node can be written as

$$\delta W_k = F_k \cdot \delta w^e(\xi = 1) \quad (53)$$

While the virtual displacement of each node is as

$$\delta w^e(\xi) = \sum_{i=1}^{N+1} \bar{H}_i^e(\xi) \delta v_i \quad (54)$$

Using Eqs. (53) and (54), the generalized force can be written as

$$\mathbf{f}_k = F_k \mathbf{\Lambda} \quad (55)$$

where, the vector $\mathbf{\Lambda}$ is defined as

$$\mathbf{\Lambda} = \begin{bmatrix} \bar{H}_1^e(\xi = 1) \\ \bar{H}_2^e(\xi = 1) \\ \vdots \\ \bar{H}_{N+1}^e(\xi = 1) \end{bmatrix} \quad (56)$$

The generalized force vector associated to a concentrated moment, M_k at the e th node can be written as

$$\mathbf{f}_k = M_k \mathbf{\Lambda} \quad (57)$$

where, the vector $\mathbf{\Lambda}$ for the moment is obtained as

$$\mathbf{\Lambda} = \begin{bmatrix} \bar{H}_1^{e'}(\xi = 1) \\ \bar{H}_2^{e'}(\xi = 1) \\ \vdots \\ \bar{H}_{N+1}^{e'}(\xi = 1) \end{bmatrix} \quad (58)$$

Furthermore, it can be shown that the generalized force vector due to a continuous force, $f(\xi)$ and a continuous moment, $M(\xi)$ in the e th element can be obtained from Eqs. (59) and (60), respectively.

$$\mathbf{f}_f = \begin{bmatrix} \int_0^1 f(\xi) \bar{H}_1^e(\xi = 1) d\xi \\ \int_0^1 f(\xi) \bar{H}_2^e(\xi = 1) d\xi \\ \vdots \\ \int_0^1 f(\xi) \bar{H}_{N+1}^e(\xi = 1) d\xi \end{bmatrix} \quad (59)$$

$$\mathbf{f}_M = \begin{bmatrix} \int_0^1 M(\xi) \bar{H}_1^{re}(\xi=1) d\xi \\ \int_0^1 M(\xi) \bar{H}_2^{re}(\xi=1) d\xi \\ \vdots \\ \int_0^1 M(\xi) \bar{H}_{N+1}^{re}(\xi=1) d\xi \end{bmatrix} \quad (60)$$

The i th column of the assembled load vectors is obtained by summation the i th column of the elements.

4.4 Natural Frequency

Using the obtained assembled mass and stiffness matrices, the dynamic equation of a beam without constraint can be written as

$$\mathbf{M}\ddot{\mathbf{v}} + \mathbf{K}\mathbf{v} = \mathbf{f} \quad (61)$$

The natural frequencies of these beams can be obtained from the following eigenvalue relation

$$|\mathbf{K} - \omega^2 \mathbf{M}| = 0 \quad (62)$$

For the beams with constraints, by incorporating the constraints, the resulting differential algebraic equations can be written as

$$\begin{bmatrix} \mathbf{M} & 0 \\ 0 & 0 \end{bmatrix} \begin{bmatrix} \ddot{\mathbf{v}} \\ \ddot{\mathbf{p}} \end{bmatrix} + \begin{bmatrix} \mathbf{K} & -\mathbf{\Gamma}^T \\ \mathbf{\Gamma} & 0 \end{bmatrix} \begin{bmatrix} \mathbf{v} \\ \mathbf{p} \end{bmatrix} = \begin{bmatrix} \mathbf{f} \\ 0 \end{bmatrix} \quad (63)$$

in which, the vector of reaction force is presented by \mathbf{p} .

The natural frequencies for these beams can be obtained by solving the following equation

$$\left| \begin{bmatrix} \mathbf{K} & -\mathbf{\Gamma}^T \\ \mathbf{\Gamma} & 0 \end{bmatrix} - \omega^2 \begin{bmatrix} \mathbf{M} & 0 \\ 0 & 0 \end{bmatrix} \right| = 0 \quad (64)$$

5 NUMERICAL EXAMPLES

In this section, some numerical examples are presented and the results are verified using DFE method. For this purpose, the beams in the presented examples are assumed to be made of steel bar of $0.1m \times 0.1m$ rectangular cross section for which $\rho = 7800 kg/m^3$ and $E = 200 GPa$. Also, the length of the beam is considered to be $\ell = 1m$.

The first five natural frequencies of the beams with different boundary conditions are obtained with DFE, CFE and CDFE methods and are shown in Table 1. The number of elements in each case is determined.

type		ω_1	ω_2	ω_3	ω_4	ω_5
Clamped-free	exact	51.39	322.09	901.86	1767.29	2921.47
	DFE(10)	51.39	322.10	902.09	1768.98	2928.83
	DFE(20)	51.39	322.09	901.88	1767.42	2921.97
	CFE(20)	51.39	322.09	901.88	1767.41	2922.04
	CDFE(10)	51.39	322.09	901.87	1767.36	2922.38
	CDFE (20)	51.39	322.09	901.86	1767.30	2922.48
Pinned-pinned	exact	144.27	577.08	1298.43	2308.32	3606.75
	DFE(10)	144.27	577.14	1299.12	2312.14	3620.99
	DFE(20)	144.27	577.08	1298.47	2308.57	3607.69
	CFE(20)	144.27	577.08	1298.47	2308.59	3608.74
	CDFE (10)	144.27	577.08	1298.45	2308.61	3609.16
	CDFE (20)	144.27	577.08	1298.43	2308.32	3606.74
Pinned-guided	exact	36.06	324.60	901.68	1767.31	2921.47
	DFE(10)	36.06	324.61	901.92	1769.04	2929.13
	DFE(20)	36.06	324.61	901.96	1767.43	2922.03
	CFE(20)	36.06	324.61	901.92	1767.21	2921.97
	CDFE (10)	36.06	324.60	901.69	1767.39	2922.37
	CDFE (20)	36.06	324.60	901.68	1767.31	2921.48
Clamped-pinned	exact	225.37	730.36	1523.85	2605.88	3976.44
	DFE(10)	225.38	730.49	1524.97	2616.37	3995.44
	DFE(20)	225.37	730.37	1523.93	2606.27	3977.92
	CFE(20)	225.37	730.37	1523.92	2606.23	3977.70
	CDFE (10)	225.37	730.36	1523.89	2606.33	3979.89
	CDFE (20)	225.37	730.36	1523.85	2605.88	3976.47
Clamped-guided	exact	81.76	441.83	1091.04	2028.80	3255.09
	DFE(10)	81.76	441.85	1091.45	2031.41	3265.66
	DFE(20)	81.76	441.83	1091.07	2028.98	3255.88
	CFE(20)	81.76	441.83	1091.07	2028.96	3255.78
	CDFE (10)	81.76	441.83	1091.05	2028.95	3256.43
	CDFE (20)	81.76	441.83	1091.04	2028.80	3255.10
Clamped-clamped	exact	327.04	901.52	1767.32	2921.47	4364.17
	DFE(10)	327.05	901.74	1769.06	2929.18	4389.14
	DFE(20)	327.04	901.52	1767.44	2922.03	4366.14
	CFE(20)	327.04	901.52	1767.43	2921.97	4365.80
	CDFE (10)	327.04	901.51	1767.43	2922.21	4369.31
	CDFE (20)	327.04	901.52	1767.32	2921.47	4364.15

Table 1: Natural frequencies of the different beam using CFE, CDFE and DFE methods.

Now, two examples for the static analysis of beams are presented. In the first example, deflection, slope and curvature distribution of a simply support beam caring a uniformly distributed load $w = 10 \text{ KN/m}$ is obtained using DFE, CFE and CDFE methods with different number of elements. The results are shown in Figures 2 to 4.

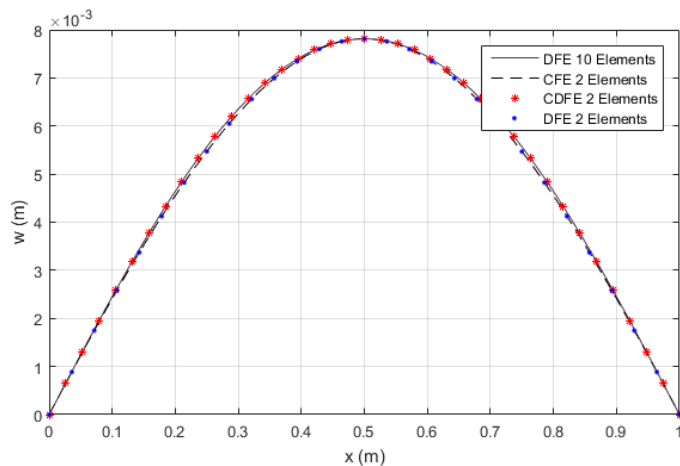


Figure 2: Deflection distribution of simply support beam using DFE, CFE and CDFE methods.

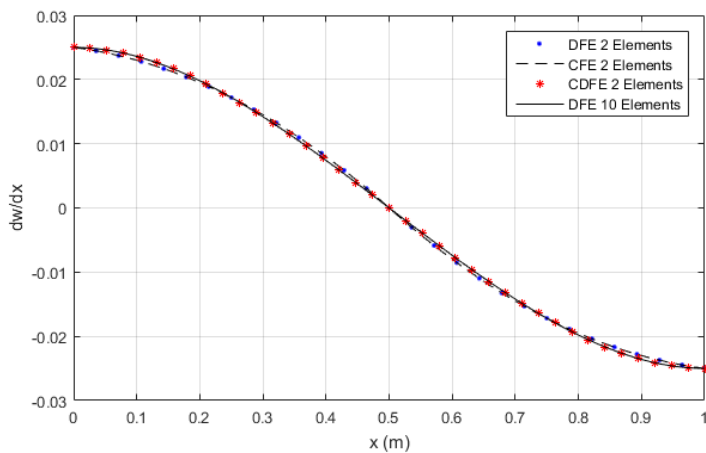


Figure 3: Slope distribution of simply support beam using DFE, CFE and CDFE methods.

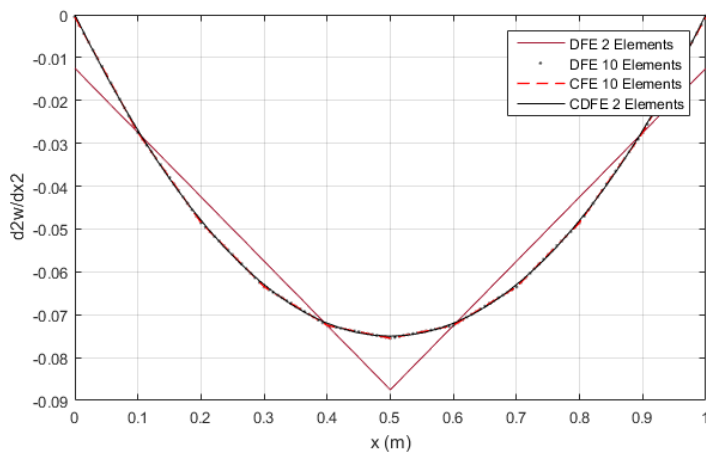


Figure 4: Curvature distribution of simply support beam using DFE, CFE and CDFE methods.

For a clamped-clamped beam with uniformly distributed load $w = 10 \text{ KN/m}$, deflection, slope and its curvature distributions are plotted in Figures 5 to 7.

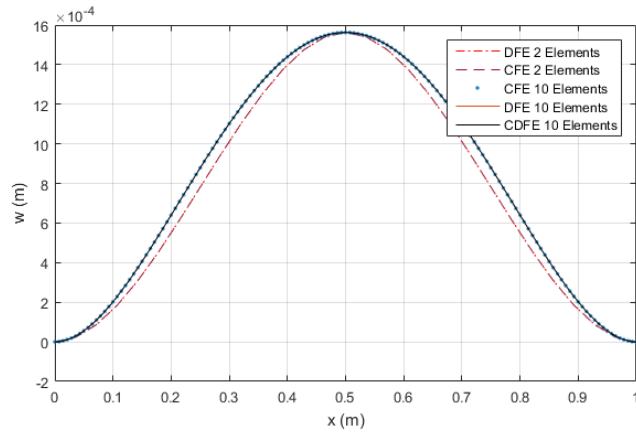


Figure 5: Deflection distribution of a clamped-clamped beam using DFE, CFE and CDFE methods.

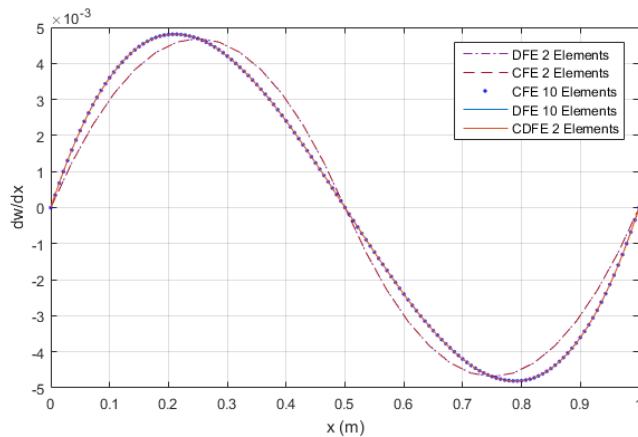


Figure 6: Slope distribution of a clamped-clamped beam using DFE, CFE and CDFE methods.

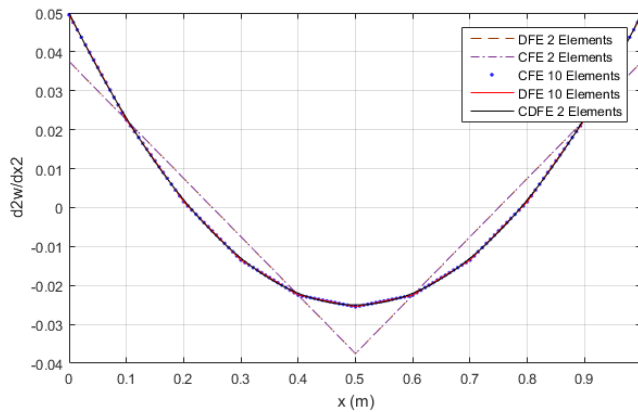


Figure 7: Curvature distribution of a clamped-clamped beam using DFE, CFE and CDFE methods.

It can be seen from Figures 2 to 7 that the deflection and slope distribution in the DFE, CFE and CDFE methods with two elements have the same accuracy. The curvature distribution in CDFE with two elements is close to the results of DFE method with ten elements which confirm the effectiveness of the CDFE method in comparison with DFE method.

Now, the dynamic response of an Euler-Bernoulli beam with CFE and CDFE methods are investigated. In the first example, midpoint deflection of a clamped free beam under a suddenly applied concentrated load $w = 10 \text{ KN}$ at point $x = 3\ell/4$ is shown in Figure 8.

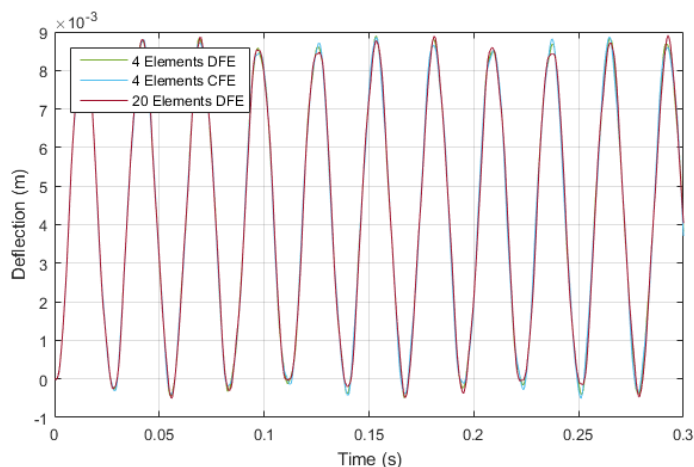


Figure 8: Midpoint deflection of a clamped-pinned beam using CFE method.

The second example is related to the dynamic response of a clamped free beam with a spring at its right end ($k = 6000 \text{ KN/m}$). The deflection of the midpoint of the beam in the presence of a suddenly distributed uniform load $w = 10 \text{ KN/m}$ is depicted in Figure 9.

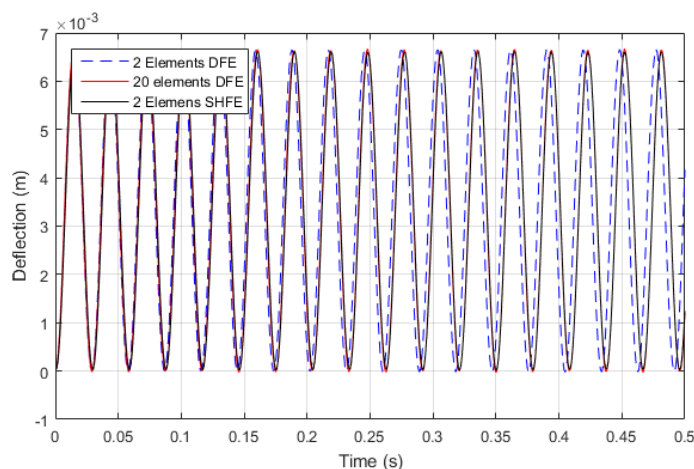


Figure 9: Midpoint deflection of the clamped-free beam using CDFE method.

As can be seen, CFE and CDFE methods have the same accuracies in comparison with DFE method. Since the number of nodal variables in CFE and CDFE methods is less than that of DFE method, the computational cost is reduced. Thus, the proposed methods are more efficient for dynamic analysis of beams and can be used for the dynamic analysis of different problems in solid mechanics.

6 CONCLUSION

This study focused on the dynamic analysis of Euler-Bernoulli beams using curvature and curvature derivative-based finite element methods. In curvature based finite element method (CFE) instead of interpolating displacement of Euler Bernoulli beam in usual displacement based finite element method (DFE), second derivative of displacement is interpolated. CFE method previously was used by a few researchers for dynamic analysis of clamped beams. In this research, CFE method was modified for static and dynamic analysis of beams with various boundary conditions.

In addition, a new method called CDFE (curvature derivative-based finite element) which is somehow a modification of CFE, was proposed. CDFE method, which interpolates the derivative of curvature instead of curvature, was used for beams with different boundary conditions.

The results were compared with those obtained by DFE method and the effectiveness of the CFE and CDFE methods was shown. In comparison with DFE method, the proposed methods have the following advantages:

- The bending moment in CFE method and the bending moment and the shear stress at the internal nodes in CDFE method are continuous.
- With fewer numbers of elastic degrees of freedom, CFE and CDFE methods are more accurate than DFE method.

References

- Chen, Z., Kong, M., Ji, C., & Liu, M. (2015). An efficient dynamic modelling approach for high-speed planar parallel manipulator with flexible links. *Proceedings of the Institution of Mechanical Engineers, Part C: Journal of Mechanical Engineering Science*, 229(4), 663-678.
- De Veubeke, B. F. (1965). Displacement and equilibrium models in the finite element method. *Stress analysis*, 9, 145-197.
- De Veubeke, B. F., Zienkiewicz, O. C. (1967). Strain-energy bounds in finite-element analysis by slab analogy. *Journal of Strain Analysis*, 2(4), 265-271.
- Farid, M., & Cleghorn, W. L. (2014). Dynamic modeling of multi-flexible-link planar manipulators using curvature-based finite element method. *Journal of Vibration and Control*, 20(11), 1682-1696.
- Farid, M., Cleghorn W. L. (2012). Dynamic Modeling of a Single-Flexible-Link Spatial Manipulator Using Curvature-Based Finite Element Method. *Proceedings of the Canadian Society for Mechanical Engineering International Congress*.
- Kuo, Y. L. (2015). Stress-based Finite Element Analysis of Sliding Beams. *Appl. Math*, 9(2L), 609-616.
- Kuo, Y. L., & Cleghorn, W. L. (2010). Curvature-and displacement-based finite element analyses of flexible four-bar mechanisms. *Journal of Vibration and Control*, 17(6), 827-844.
- Kuo, Y. L., Cleghorn, W. L. (2007, June). Application of Stress-based Finite Element Method to a Flexible Slider Crank Mechanism. In 12th IFToMM Congress, Besancon, France.

Kuo, Y. L., Cleghorn, W. L., & Behdinan, K. (2006). Stress-based finite element method for Euler-Bernoulli beams. Transactions of the Canadian Society for Mechanical Engineering, 30(1), 1-6.

Morley, L. S. D. (1968). The triangular equilibrium element in the solution of plate bending problems. Aeronautical Quarterly, 19(02), 149-169.

Punch, E.F., Atluri, S.N. (1986). Large displacement analysis of plates by stressed-based finite element approach. Computers and Structures, 24(1), 107-117.

Watwood, V. B., & Hartz, B. J. (1968). An equilibrium stress field model for finite element solutions of two-dimensional elastostatic problems. International Journal of Solids and Structures, 4(9), 857-873.

Wieckowski, Z. (1995). Dual finite element analysis for plasticity–friction torsion of composite bar. International journal for numerical methods in engineering, 38(11), 1901-1916.

Więckowski, Z., Youn, S. K., & Moon, B. S. (1999). Stress based finite element analysis of plane plasticity problems. International journal for numerical methods in engineering, 44(10), 1505-1525.

APPENDIX

The first five Shape functions of Euler-Bernoulli beam for CFE and CDFE methods are presented in the following table.

Element 1	Element 2	Element 3	Element 4	Element 5
$H_1^1 = h^2(\frac{\xi^2}{2} - \frac{\xi^3}{6})$	$H_1^2 = h^2(\frac{1}{2}\xi + \frac{1}{3})$	$H_1^3 = h^2(\frac{1}{2}\xi + \frac{5}{6})$	$H_1^4 = h^2(\frac{1}{2}\xi + \frac{8}{6})$	$H_1^5 = h^2(\frac{1}{2}\xi + \frac{11}{6})$
$H_2^1 = h^2(\frac{\xi^3}{6})$	$H_2^2 = h^2(\xi + 1)$	$H_2^3 = h^2(\xi + 1)$	$H_2^4 = h^2(\xi + 2)$	$H_2^5 = h^2(\xi + 3)$
$H_3^1 = 0$	$H_3^2 = h^2(\frac{\xi^3}{6})$	$H_3^3 = h^2(\frac{1}{2}\xi + \frac{1}{6} + \frac{\xi^2}{2} - \frac{\xi^3}{6})$	$H_3^4 = h^2(\xi + 1)$	$H_3^5 = h^2(\xi + 2)$
$H_4^1 = 0$	$H_4^2 = 0$	$H_4^3 = h^2(\frac{\xi^3}{6})$	$H_4^4 = h^2(\frac{1}{2}\xi + \frac{1}{6} + \frac{\xi^2}{2} - \frac{\xi^3}{6})$	$H_4^5 = h^2(\xi + 1)$
$H_5^1 = 0$	$H_5^2 = 0$	$H_5^3 = 0$	$H_5^4 = h^2(\frac{\xi^3}{6})$	$H_5^5 = h^2(\frac{1}{2}\xi + \frac{1}{6} + \frac{\xi^2}{2} - \frac{\xi^3}{6})$
$H_6^1 = 0$	$H_6^2 = 0$	$H_6^3 = 0$	$H_6^4 = 0$	$H_6^5 = h^2(\frac{\xi^3}{6})$

Table 2: Shape functions (CFE).

Element 1	Element 2	Element 3	Element 4	Element 5
$H_1^1 = h^3(\frac{\xi^3}{6} - \frac{\xi^4}{24})$	$H_1^2 = h^3(\frac{\xi^2}{4} + \frac{1}{3}\xi + \frac{1}{8})$	$H_1^3 = h^3(\frac{\xi^2}{4} + \frac{5}{6}\xi + \frac{17}{24})$	$H_1^4 = h^3(\frac{\xi^2}{4} + \frac{4}{3}\xi + \frac{43}{24})$	$H_1^5 = h^3(\frac{\xi^2}{4} + \frac{11}{6}\xi + \frac{27}{8})$
$H_2^1 = h^3\frac{\xi^4}{24}$	$H_2^2 = h^3(\frac{1}{24} + \frac{1}{6}\xi + \frac{\xi^2}{4} + \frac{\xi^3}{6} - \frac{\xi^4}{24})$	$H_2^3 = h^3(\frac{\xi^2}{4} + \xi + \frac{7}{12})$	$H_2^4 = h^3(\frac{\xi^2}{4} + 3\xi + \frac{55}{12})$	$H_2^5 = h^3(\frac{\xi^2}{4} + 3\xi + \frac{55}{12})$
$H_3^1 = 0$	$H_3^2 = h^3(\frac{\xi^4}{24})$	$H_3^3 = h^3(\frac{1}{24} + \frac{1}{6}\xi + \frac{\xi^2}{4} + \frac{\xi^3}{6} - \frac{\xi^4}{24})$	$H_3^4 = h^3(\frac{\xi^2}{4} + \xi + \frac{14}{24})$	$H_3^5 = h^3(\frac{\xi^2}{4} + 2\xi + \frac{25}{12})$
$H_4^1 = 0$	$H_4^2 = 0$	$H_4^3 = h^3(\frac{\xi^4}{24})$	$H_4^4 = h^3(\frac{1}{24} + \frac{1}{6}\xi + \frac{\xi^2}{4} + \frac{\xi^3}{6} - \frac{\xi^4}{24})$	$H_4^5 = h^3(\frac{\xi^2}{4} + \xi + \frac{14}{24})$
$H_5^1 = 0$	$H_5^2 = 0$	$H_5^3 = 0$	$H_5^4 = h^3(\frac{\xi^4}{24})$	$H_5^5 = h^3(\frac{1}{24} + \frac{1}{6}\xi + \frac{\xi^2}{4} + \frac{\xi^3}{6} - \frac{\xi^4}{24})$
$H_6^1 = 0$	$H_6^2 = 0$	$H_6^3 = 0$	$H_6^4 = 0$	$H_6^5 = h^3(\frac{\xi^4}{24})$

Table 3: Shape functions (CDFE).